RSC Advances

ROYAL SOCIETY OF CHEMISTRY

www.rsc.org/advances

Journal Name

ARTICLE

Preparation of N-doped activated carbons with high CO_2 capture performance from microalgae (*Chlorococcum sp.*)

Received 00th January 20xx,
Accepted 00th January 20xx

DOI: 10.1039/x0xx00000x

www.rsc.org/

H. Luo,[a] C.C. Zhu,[a] Z.C. Tan,[a, b] L.W. Bao,[a, b] J.J. Wang,[a] G. Miao,[a] L.Z. Kong*[a] and Y.H. Sun*[a,c]

N-doped activated carbons with high CO_2 adsorption capacity have been prepared from sugar-rich microalgae (*Chlorococcum sp.*) feedstock via simple hydrothermal carbonization coupled with KOH activation or NH_3 modification. The KOH activated carbons exhibit higher CO_2 capture performance compared with the ones treated by NH_3. The nitrogen-enriched hydro-char derived from microalgae was activated with KOH at 700°C to improve the textural characteristics (surface area, pores size, and total pore volume), and the resulting carbon showed a highly ordered structure with the surface area of 1745 m^2/g, and narrow pore size distribution with the maxima peak located in the micropore range (<1.0 nm). The activated carbon exhibited CO_2 uptakes of 4.03 and 6.68 mmol/g at 25°C and 0°C, respectively. Further XPS analysis revealed the effective pyridonic-nitrogen species (up to 58.32%) on the carbon surface favored a higher CO_2 capture capacity. The N-doped activated carbons displayed rapid adsorption kinetics with ultrahigh selectivity for CO_2 over N_2 (up to 11 at 25°C), and no obvious decrease in the CO_2 uptake capacity was observed even after seven times cycles, which may be due to the dominant physisorption between CO_2 and the surface of carbon.

1. Introduction

Emission of CO_2 gas has caused serious environmental problems such as global climate change and acidification of oceans, since CO_2 is generally recognized as the main greenhouse gas and contributes to nearly 60% of global warming effects [1-2]. Carbon capture and storage (CCS) has been proposed as a prevailing method for reducing CO_2 emissions [3-4]. Amine scrubbing is a widely used traditional technology to capture and isolate CO_2 from fossil-fuelled power plants. However, this process suffers from many issues, such as high energy consumption for regeneration, solvent loss, toxicity and equipment corrosion [5]. To address these challenges, adsorption using porous solids as sorbents is regarded as a promising alternative technology.

To date, intensive researches have focused on the preparation of efficient porous solids, including porous carbons [6-7], zeolites [8], metal-organic frameworks (MOFs) [9-11], covalent organic frameworks (COFs) [12], and nitrogen-rich porous polymers [13,14]. Among the sorbents mentioned above, porous carbons are especially attractive because they have several advantages such as low-cost and easy preparation, high thermal and chemical stability, easy-to-design pore structure and ease of regeneration [15, 16].

In order to further enhance the CO_2 adsorption capacity and selectivity, some new functional groups, particularly nitrogen functionalities, have been introduced into porous carbons. Generally, there are two methods for adding nitrogen functionalities into carbon framework. The first one is post-synthesis via the treatment with ammonia, melamine and urea or the way of carbon impregnation (e.g., PEI, diamines). Shafeeyan et al. [17] confirmed that the CO_2 adsorption capacity of a commercial activated carbon was enhanced when it was subjected to high temperature ammonia treatment, due to introducing basic nitrogen functionalities on the carbon surface. Bai et al. [16] synthesized a highly-efficient carbonaceous CO_2 sorbent using inexpensive urea to modify petroleum coke. The CO_2 adsorption capacity of the resulting carbon reached 4.40mmol/g under 1 bar at 25°C and the CO_2/N_2 selectivity of the sorbent was 17. Grondein et al. [18] used diamines to modify carbon black by an impregnation method. The presence of amine groups provided better selectivity towards CO_2 adsorption, but resulting in a lower maximum CO_2 uptake compared to unmodified carbon. The second strategy is via the direct pyrolysis of N-containing precursors during the preparation of N-doped carbons. Wang et al. [13] prepared hierarchical mesoporous/microporous nitrogen-rich polymer networks, using melamine, resorcinol and terephthaldehyde as precursors. The CO_2 adsorption capacity reached 2.4mmol/g at 25°C, at 1 atm. Sevilla et al. reported polypyrrole-based porous carbons with 10.1 bulk wt% N via one-pot chemical activation of polypyrrole with KOH, which showed a high CO_2 adsorption uptake of 6.2 mmol/g (0°C, 1atm), large kinetic selectivity of 5.3 and rapid adsorption-desorption rates at 25°C [19]. Hao et al. [20] presented a facile approach for synthesizing a porous

[a] CAS Key Laboratory of Low-Carbon Conversion Science and Engineering, Shanghai Advanced Research Institute, Chinese Academy of Sciences, Shanghai 201210, PR China. E-mail: konglz@sari.ac.cn, sunyh@sari.ac.cn
[b] University of Chinese Academy of Sciences, Beijing 100049, PR China.
[c] School of Physical Science and Technology, Shanghai-Tech University, Shanghai 200031, PR China.

carbon monolith, using L-lysine as both catalyst and nitrogen source and obtained a maximum CO_2 adsorption capacity of 3.13mmol/g at 25°Cunder ambient pressure. Obviously, these results have pointed out introducing nitrogen-containing functionalities into the surface of porous carbons is beneficial for the enhancement of CO_2 adsorption capacity or selectivity, regardless of which ways the nitrogen sources were introduced.

Taking into account the potential scale and sustainable factors involved in the production of porous carbons for CO_2 capture, the use of renewable sources for fabricating these materials would be highly desirable. Xing et al. [21] used bean dreg (a biomass waste) as director precursor and prepared a series of N-enriched activated carbons by the direct pyrolysis, which possess an unprecedented CO_2 uptake capacity of 4.24mmol/g under 1atm at 25°C. Compared with the dry pyrolysis of biomass precursors, the hydrothermal carbonization (HTC) of protein-rich biomass has a higher nitrogen content and carbon yield and can directly handle the wet biomass, which has been proven to be a new and effective alternative pathway for preparing homogeneously N-doped carbon. For example, a protein-rich biomass (*a marine macroalgae*) from an ocean pollutant was used to synthesize nitrogen-containing carbon via hydrothermal carbonization and KOH activation, which performed high CO_2 capacity and facile regeneration at room temperature [22]. In addition, nitrogen-containing monosaccharides/polysaccharides or mixtures of amino acids (e.g., proteins) and sugars have been successfully used as precursors to N-doped carbons [23, 24]. Microalgae, a kind of single-celled aquatic plant with very high photosynthesis efficiency and fast growth rate, is primarily composed of proteins, carbohydrates, lipids and nucleic acids [23, 25]. In general, the proportion of each component is varied by species. These characteristics make microalgae attractive precursors for the production of carbon materials. However, researches and applications about microalgae were mainly focused on the bio-fuel production, eutrophic wastewater purification and bio-chemicals [25, 26]. To date, there have been only a few studies on the direct use of algae or microalgae for producing carbons materials [25-28], and the exploitation of utilizing microalgae with high nitrogen content as precursor to produce N-containing carbons materials for carbon capture and storage (CCS) has been scarce [29].

Herein, we present a novel, low-cost route for synthesizing a series of N-doped activated carbons derived from sugar-rich microalgae. To fully take advantage of the high carbohydrate and Nitrogen (protein) content of microalgae, we firstly obtained a nitrogen-enriched hydro-char through hydrothermal carbonization, and then chemical activation using KOH or NH_3 under varying conditions. Our results show that these N-doped activated carbons exhibit a maximum CO_2 adsorption capacity of 4.03 mmol/g and 6.68 mmol/g at 25°C and 0°C under atmospheric pressure (1bar), respectively. This study further focuses on the relationship between the porous structures, nitrogen-containing group and their high CO_2 adsorption capacity of carbon materials.

2. Experimental

2.1 Materials

The microalgae (*Chlorococcum sp.*) used in this study were self-cultured by our collaborators. The comprehensive compositions of microalgae were shown in Table 1. The main component of the microalgae was carbohydrate (up to 49.6%), which means the microalgae in this study was a special sugar-rich species. All the other chemicals were purchased from Sinopharm Chemical Reagent Co., Ltd, and used as received without further purification.

Table 1 Characterization of microalgae (*Chlorococcum sp.*).

Biochemical composition (wt %)	Elemental analysis (wt %)
Carbohydrate : 49.6	C : 48.4
Lipid : 32.6	O : 42.0
Protein : 11.9	H : 7.6
Moisture + Ashes : 5.9	N : 1.9
	S : 0.1

2.2 Synthesis of N-doped activated carbons

The N-doped hydro-char was prepared by hydrothermal carbonization of microalgae (*Chlorococcum sp.*). Briefly, 6.0 g of microalgae and 30 ml distilled water were placed in a stainless steel autoclave (Parr Rector, 100 ml), heated up to 200°C and maintained at this temperature for 3 h. After the reaction, the autoclave was allowed to cool down to room temperature. The resulting solid products, denoted as hydro-char, were collected by filtration, washed with distilled water and finally dried at 110 °C for 12 h.

In this study, hydro-char materials underwent two different chemical modifications, direct KOH activation and NH_3 activation, respectively. Typically, 2 g hydro-char was mixed with 4 g KOH and 20 ml distilled water and stirred at 600 rpm for 4 h, followed by another 16 h of static soaking under ambient conditions. After drying overnight at 120 °Cin an oven, the mixture was first heated to 400°C with a retention time of 30 min at heating rate of 8°C/min, and then to target temperature (650-750°C) with a retention time of 60 min at 10°C/min under flowing N_2 (120 ml/min，gas purity 99.99%). After cooling down naturally, the sample was repeatedly washed by distilled water until a pH value of 7 was reached. The activated carbons thus synthesized were denoted as KC-x, where x refers to the activation temperature (°C). For a direct NH_3 activation, the hydro-char was subjected to a second heat treatment under flowing NH_3 (100ml/min，gas purity 99.99 %) at 900°C for 30min to form the NH_3 activated carbon. It must be noted that the heating and cooling steps were performed in N_2 atmosphere (N_2 flowing rate of 120 ml/min). As is similar with above, carbons by NH_3 activation were denoted as NC-y, where y refers to the activation temperature (°C). Finally, we also synthesized the third kind of carbon, which meant the hydro-char was firstly activated by KOH and then followed by NH_3. This kind of carbon was denoted as KNC-x-y, where x refers to the KOH activation temperature and y the NH_3 activation temperature (°C).

2.3 Characterization

The morphology of the samples was examined by Scanning Electron Microscopy (SEM) using S-4800 instrument. Elemental analysis (C, H and N) was performed on a dry basis using a Thermo Scientific Flash 2000 analyzer. Nitrogen sorption isotherms and textural properties of samples were measured on Micromeritics ASAP 2020 equipment at liquid nitrogen temperature. Before measurement, the samples were degassed in a vacuum at 200°C for at least 12h. X-ray photoelectron (XPS) was carried out by means of an AXIS Nova spectrometer (Kratos Inc., NY, USA) equipped with monochromatic Al Kα radiation (186.6 eV). Binding energies for the high resolution spectra were calibrated by setting N 1s at 400 eV.

2.4 CO_2 adsorption and desorption measurements

CO_2 and N_2 adsorption isotherms were measured using a Micromeritics ASAP 2020 static volumetric analyzer at 0°Cand 25°C within the pressure range from 0.01~1 bar. Prior to each adsorption analysis, the samples were degassed at 200°C for several hours. The adsorption kinetics of the CO_2 and N_2, and adsorption-desorption cycles were measured in an Intelligent Gravimetric Analyzer (IGA). Both sets of experiments were performed at 25°C and the temperature was controlled by means of a circulating bath. For the kinetics analysis, the sample (≈30mg) was degassed under vacuum at 200°C for at least 4 h. Then the pressure of CO_2 or N_2 was changed gradually from 10~1000 mbar and the weight variation with time was recorded. In the case of the adsorption-desorption cycles, the sample (≈30mg) was also degassed under vacuum at 200°C for several hours. During the adsorption, the pressure of CO_2 was changed gradually from 10~1000 mbar. Once the sample was saturated, the instrument automatically discharged the gas to a pressure below 10 mbar for CO_2 desorption. The sample was kept under vacuum for 10 min, and then allowed to adsorb CO_2 again. This adsorption-desorption cycle was repeated seven times.

3. Results and Discussion

3.1 Structural Characteristics of the Porous Carbons

In order to reveal the morphology changes of the carbons clearly, scanning electron microscopy (SEM) was used to observe the hydro-char and three different kinds of activated carbons. The panoramic image of hydro-char (in Fig.1a) exhibits irregular shaped bulks with some disorder accumulations. While after chemical activation with KOH, the SEM image for the KC-700 sample clearly demonstrates the formation of irregular and macro-porous networks (in Fig.1b). The drastic morphological change has been proved the KOH activation is an effective approach. Compared with KC-700, the image of KNC-650-900 has no obvious difference (in Fig.1d). In contrast, the NC-900 sample which was directly activated by NH_3 shows a great number of spherical particles (in Fig.1c).

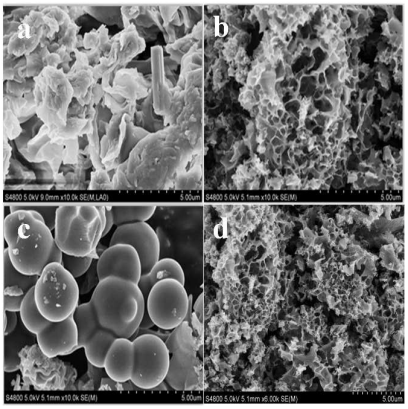

Fig. 1 SEM images of a) hydro-char, b) KC-700, c) NC-900, d) KNC-650-900.

The porosity of the activated materials was examined through N_2 sorption at -196°C. As shown in Fig.2a, all carbons except for NC-900 and KC-650 show a combination of type I and type IV isotherms, which presents both a sharp increase at low relative pressure (p/p_0<0.05), revealing the presence of micropores, and a conspicuous H4 hysteresis loop with a high relative pressure range (p/p_0=0.45~1.0), and indicating the presence of mesopores structure. It must be noted that macroporous structures also exist in these activated carbons with increasing N_2 adsorption when the relative pressure P/P_0 approaches to 1.0. In contrast, KC-650 and NC-900 exhibit typeI, typical of microporous material. The adsorption and desorption branches of the isotherms fit very well without any hysteresis loops. A large adsorption uptake of the isotherms represents micropores filling and the plateau indicates multilayer adsorption on the external surface.

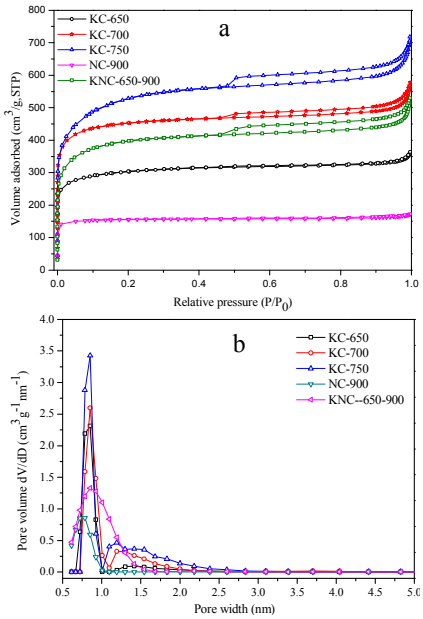

Fig.2 (a) N_2 sorption isotherms and (b) pore size distribution of the porous carbons with DFT method prepared at different conditions.

The detailed textural parameters of these porous carbons are given in Table 2. It can be seen that the hydro-char has low total surface area ($11 m^2/g$) and negligible pore volume, which is consistent with other hydrothermally treated hydro-char of biomass [22, 30]. It should be noted that, for all KOH activation carbons the specific surface area and total pore volume increase with the rise of activation temperature, with values ranging from 1151 m^2/g (650°C) to 1959 m^2/g (750°C) and from 0.71 cm^3/g (650°C) to 1.10 cm^3/g (750°C), respectively. However, the fraction of micropore volumes to total pore volumes (V_n) follow the opposite trend, with values ranging from 83.9% to 72.7%, suggesting that more mesoporous and macroporous structures were generated or partial micropores were destroyed at high temperature due to over-activation. Compared with KOH activation carbons, the NC-900 sample has a relative low specific surface area and total pore volume, but a very high ratio of micropore volumes to total pore volumes, whose proportion is as high as 88.9%. In relation to KC-650 sample, both the specific surface area and total pore volume of KNC-650-900 sample increase to some extent, whereas the values of V_n decrease from 83.9% to 73.2%, indicating the porosity of KC-650 sample has been further developed when it was treated with NH_3 at elevated temperature.

Table 2 Textural properties of porous carbons.

Samples	S_{BET} (m^2/g)	S_{micro}[a] (m^2/g)	V_t[b] (cm^3/g)	V_{Micro}[c] (cm^3/g)	V_n[d] (%)	Pore Size (nm)
Hydro-char	11	-	-	-	-	-
KC-650	1151	1110	0.56	0.47	83.9	0.82/1.25
KC-700	1745	1677	0.89	0.69	77.5	0.82/1.25
KC-750	1959	1850	1.10	0.80	72.7	0.82/1.25
NC-750	621	615	0.27	0.24	88.9	0.73
KNC-650-900	1509	1435	0.82	0.60	73.2	0.82

[a]Micropore surface area determined by thet-plot method.

[b]Total pore volume at p/p_0~0.99.

[c]Micropore volume calculated by the t-plot method.

[d]$V_n=V_{Micro}/V_t$.

The pore size distribution (PSD) curves of the porous carbons prepared at different conditions are presented in Fig. 2b, which indicate that the porous carbons possessed micropores and mesopores, and further confirm the presence of a hierarchical porous structure. The PSD curves contain two peaks at about 0.82 and 1.25 nm, representing the volume of different micropores (denoted as $V_{0.82}$ and $V_{1.25}$). The $V_{0.82}$ and $V_{1.25}$ increase with the increasing of activation temperature, indicating that the micropores of microalgae derived activated carbons were enlarged. The samples prepared at higher activation temperature had much larger micropores ($V_{1.25}$), and suffered greater loss of their adsorbed amounts of CO_2 when the adsorption temperatures increased from 0 to 25 °C (Fig. 4d), showing the larger micropores were unsuitable for CO_2 adsorption. The sample KC-700 had a larger volume of small micropores ($V_{0.82}$) and a relatively small volume of large micropores ($V_{1.25}$), resulting in the highest CO_2 adsorption at the temperatures from 0 to 25 °C among all the samples. The sample NC-900 and KNC-650-900 derived from NH_3 activation showed a wide range of micropores at 0.7~1.0 nm and 0.7~1.5nm, indicating that nitrogen modification process on the carbon surface had a great effect on the generation of microporous channels. So, the method of chemical modify-cations of microalgae had significant effects on the PSD of porous carbons. For the sugar-rich microalgae we used, which had the potential to obtain carbon microspheres with high surface area and good sphericity under HTC process, and could offer a large volume of micropores in a narrow range with only KOH activation.

3.2 Chemical Properties of N-Doped activated Carbons

Elemental compositions of the raw material and the prepared carbons are included in Table 1 and Table 3. The hydrothermal carbonization treatment of the microalgae leads to increasing both carbon and nitrogen retention in the final hydro-char product, which exhibits the values of carbon content ranging from 48.40% to 66.86% and nitrogen contents from 1.90% to 3.32%. During the hydrothermal carbonization, Maillard-type cascade reactions takes place between the amino groups in amino acids and the carbonyl moieties present in carbohydrates and their derivatives (e.g., HMF) [24], resulting in the enrichment of carbon and nitrogen. Further KOH activation of hydro-char has caused a sharp decrease in nitrogen amounts, which is due to the reaction or pyrolysis of some unstable nitrogen groups during the chemical activation. The carbon content increases from 66.86% to 85.08% after KOH activation, indicating a deeper graphitization was formed as the activation temperature increase. It is known to us, NH_3 was generally recognized as a nitrogen precursor for preparing N-doped carbon catalysts [17, 31-32]. Actually, the final nitrogen content of NC-900 (4.59%) obtained with NH_3 activation was significantly higher than that of hydro-char (3.32%). Simultaneously, the nitrogen content of sample KNC-650-900 increased from 1.42% for KC-650 to 2.57%, which clearly confirming the nitrogen groups can be successfully introduced to carbon surface after treatment of NH_3.

Table 3 Elemental composition and surface chemical properties of the raw material and prepared carbons.

Sample	C[a] (wt %)	H[a] (wt %)	N[a] (wt %)	N-5[b] (%)	N-6[b] (%)	N-Q[b] (%)
Hydro-char	66.86	6.66	3.32	100	0	0
KC-650	75.62	0.93	1.42	46.75	24.17	29.08
KC-700	79.04	0.86	1.15	58.32	9.42	32.26
KC-750	85.08	0.73	1.00	48.58	5.52	45.90
NC-900	79.48	1.05	4.59	33.67	39.41	26.92
KNC-650-900	80.36	0.85	2.57	39.39	25.81	34.80

[a]Elemental analysis.

[b]X-ray photoelectron spectroscopy data.

Except for elemental compositions, XPS analysis also provided valuable information concerning the nature of chemical bonds present on the carbon surface. Herein, we paid special consideration to nitrogen species since they have been shown to be vital for improving the CO_2 adsorption capacity. Fig.3 shows the N1s XPS spectra of representative samples, i.e. Hydro-char,

KC-650, NC-900 and KNC-650-900. The peaks at 398.1~398.3, 400.1~400.5 and 401.5 eV are attributed to pyridinic-N (N-6), pyrrolic-/pyridonic-N (N-5) and quaternary-N (N-Q), respectively. Although pyrrolic-N and pyridonic-N are indistinguishable by XPS, taking into account the conditions of the activation process, e.g. oxidative environment and high temperatures (>650°C), the peak at 400.1~400.5eV is most likely attributed to pyridone-type structures [19, 33]. The quantitative analysis of each kind of nitrogen-containing group was given in table 3. It obviously reveals that the relative amount of pyridonic-N (N-5) is higher than that present in the form of N-6 and N-Q for all activated carbons (except NC-900 sample). This feature is particularly noticeable for the KC-700 sample, which displays about 58% of N-5, against only 33%~48% for other samples. Interestingly, compared with carbons by KOH activation, although the NC-900 and KNC-650-900 samples contain more total nitrogen content, they have the lower relative amount of pyridonic-nitrogen (N-5) species and higher pyridinic-N (N-6) containing. This may be relevant to the CO_2 capture, since it has documented that pyridonic nitrogen (N-5) species plays a more important role in CO_2 capturing than pyridinic nitrogen and quaternary nitrogen [16, 19, 34].

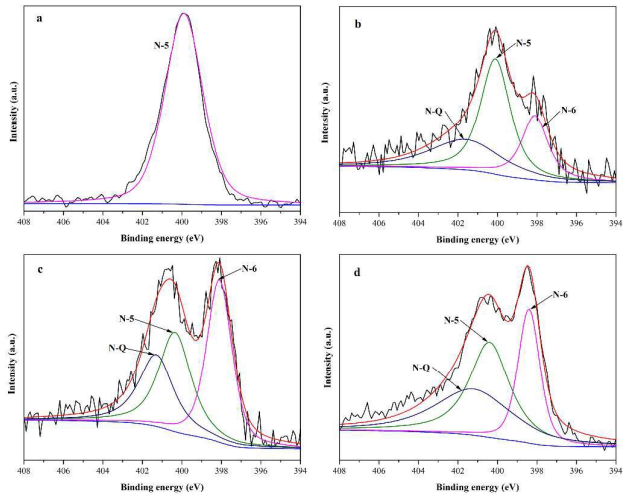

Fig.3 XPS spectra of the raw material and activated carbons: (a) Hydro-char, (b) KC-650, (c) NC-900, (d) KNC-650-900.

3.3 CO_2 Capture Capacity

CO_2 adsorption behaviors on different carbonaceous materials have been investigated at 25°C and 0°C under sub-atmospheric pressure (up to 1 bar). The CO_2 adsorption isotherms and isosteric heat of adsorption are shown in Fig. 4. It can be clearly seen that CO_2 capture capacities of the prepared carbons treated by different ways are quite different. This result clearly demonstrated that N-doped activated carbons derived from microalgae were excellent sorbents for CO_2, which was comparable to the porous carbons derived from sustainable biomass product [7, 19]. Figure 4a showed the difference of CO_2 uptakes between the 5 carbon samples (treated by different ways). KC-700 held the highest CO_2 capture capacity, followed by KC-650 and KC-750, which did not match the trend of micropore volumes for different samples. It should be noted that, for all KOH activation carbons, the micropore volume increase with the rise of activation temperature, with values ranging from 0.47 cm^3/g (650°C) to 0.80 cm^3/g (750°C), while the nitrogen content of the samples decreased from 1.42% to 1.00%. It was obvious that nitrogen played a role in the adsorption of CO_2 for carbon materials, and could further enhance the CO_2 adsorption capacity and selectivity in a certain extent.

From the adsorption isotherms at 0 °C and 25°C, the isosteric heat values of CO_2 adsorption (Q_{st}) on the N-doped activated carbons were calculated by the Clausius-Clapeyron equation (Fig.4c). The Q_{st} values decreased from 31.5 kJ/mol to 22.4 kJ/mol when adsorption capacity of CO_2 increased from 0.25 mmol/g to 4.0 mmol/g, which was identified that the physisorption took place dominantly between CO_2 and the N-doped active carbons. The variation of Q_{st} values with the increasing of CO_2 loading may be due to heterogeneity of adsorption sites and also variation in adsorbate-adsorbent interactions. The high Q_{st} in the initial stage lead to a preferential adsorption of CO_2, which may be attributed to the large amount of micropores in the samples.

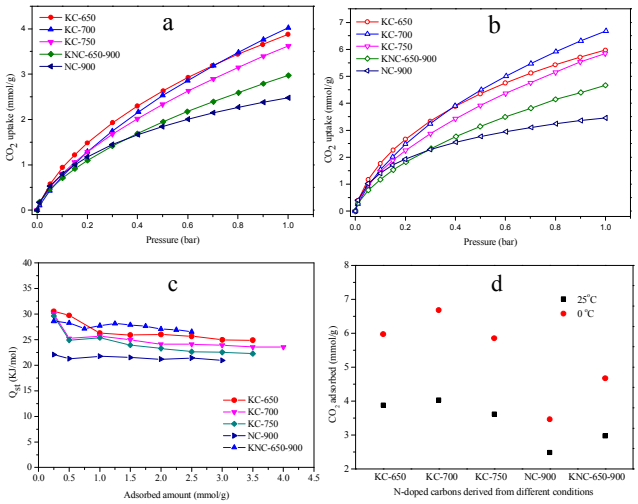

Fig.4 CO_2 adsorption isotherms of N-doped carbons at (a) 25°C and (b) 0°C, (c)Isosteric heat of adsorption (d) adsorbed amount of CO_2 for different samples

CO_2 adsorption on the N-doped active carbons are mainly dependent on physical adsorption, which is mostly contributed by textural characteristics of micropores and the interaction between functional groups and CO_2 molecules on the external surface. For the low porosity samples, limited pore structure and amino groups exposed on surface resulted in a low CO_2 capture capacity. For the activated samples with rich pore channels, such as high specific surface area and pore volume, which may not only facilitate the formation of more surface-exposed amine groups but also accelerate the diffusion of CO_2 into carbon matrix more rapidly, thus increasing the physical adsorption of CO_2. Moreover, all the KOH activation carbons

which contained the lowest total nitrogen content (1.0~1.4wt%), exhibited excellent CO_2 capture capacities, with values ranging from 3.62 to 4.03mmol/g CO_2 at 25°C and from 5.85 to 6.68mmol/g CO_2 at 0°C (Fig. 4d), while the samples obtained under NH_3 activation conditions (i.e. NC-900 and KNC-650-900 whose nitrogen contents are up to 4.59wt% and 2.57wt% respectively) had lower CO_2 uptakes.

This can be explained by the two following reasons: (1) the micropore volume or narrow micropores (<1nm) play a dominant role in CO_2 filling due to high adsorption potential. (2) CO_2 capture performance is also dependent on the relative proportion of doped pyridonic-nitrogen (N-5) rather than the total amount of nitrogen species. Apparently, the KOH activation samples had the higher micropore volumes (in Table 2) and the relative proportions of N-5 (in Table 3) than NC-900 or KNC-650-900 samples. Interestingly, the KC-650 sample showed an obvious change in the porosity and nitrogen content when it was further activated by NH_3. Compared with KC-650, although KNC-650-900 developed pore structure and increased nitrogen content, it reduced the microporous volume and the relative ratio of N-5 species, finally decreasing the CO_2 capacity. Therefore, the key points for improving CO_2 adsorption ability of these N-doped carbons should be both introduced the amount of effective nitrogen, such as the proportion of N-5 species on the surfaces, and developed micro-porosity structures, especially the micropores in a narrow range, which will help the design of high performance CO_2 capture materials.

3.4 Kinetics of Adsorption, (CO_2/N_2) Selectivity and Sorbent Regeneration

In addition to large CO_2 uptake capacity, a fast adsorption kinetics and good selectivity against other molecules in the flue gas (*i.e.* N_2) and easy regeneration of adsorbents are another three critical factors that must be considered when selecting an effective and economic adsorbent material. Fig.5a presents the adsorption kinetics curves of CO_2 and N_2 over the KC-700 sample at 25°C. These measurements were carried out in an IGA system, as described in the experimental section. It can be noted that the CO_2 adsorption rate is fast with around 95% of CO_2 uptake being obtained within 2.5 min, around 6 min was needed to achieve the adsorption equilibrium. However, at same conditions N_2 adsorption needs only 50 seconds to reach the saturation level, which is much quicker than CO_2 adsorption. This finding implies that high CO_2/N_2 selectivity can be achieved for short adsorption times. In fact, the selectivity of KC-700 sample for CO_2 over N_2 was determined by recording single-component isotherms of CO_2 and N_2 under the same experimental conditions, and the details were showed in Fig.5b. Selectivity of CO_2 over N_2 was calculated using Henry's Law through the initial slopes of CO_2 and N_2 adsorption isotherms. Finally, the estimated CO_2/N_2 selectivity of KC-700 sample is 11, which is comparable to the recently reported nitrogen-doped carbons [7, 16, 19, 35-36], in which CO_2/N_2 selectivity is also calculated using the same method described above.

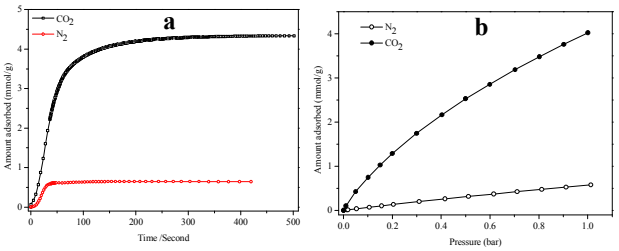

Fig.5 Adsorption kinetics (a) and isotherms (b) of CO_2 and N_2 for the KC-700 sample at 25°C under pressure 0~1 bar.

To test the reusability of the carbon sorbents, adsorption-desorption cycles of the representative sample KC-700 were performed at 25°C in an IGA system. As shown in Fig. 6, both CO_2 adsorption and desorption processes are very fast, taking place in a span of 10 min. Furthermore, no noticeable decrease in the CO_2 uptake capacity was observed even after seven times cycles, which may be due to the dominant physisorption between CO_2 and N-doped active carbon. In short, these results obviously reveal that the porous carbons reported here are highly stable for practical applications and can be easily, quickly and totally regenerated over multiple cycles without any significant loss in the CO_2 capture performance.

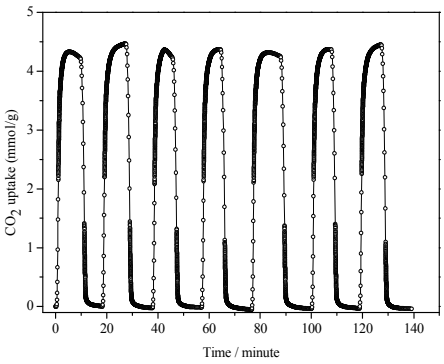

Fig.6 CO_2 adsorption-desorption cycles for KC-700 sample at 25°C and 1 bar.

Conclusions

The sugar-rich microalgae (*Chlorococcum sp.*) could provide low-cost and high CO_2 adsorption capacity N-doped activated carbons through the hydrothermal carbonization and a subsequent step of KOH or NH_3 activation under varying conditions. The results showed that porous carbons using KOH activation exhibited a higher CO_2 adsorption capacity than that treated by NH_3. Specifically, the sample KC-700 exhibited high CO_2 uptakes of 4.03mmol/g at 25°C and 6.68mmol/g at 0°C, respectively. The superior CO_2 capture capacity is due to the high volume and narrow range of micropores and the proportion of effective nitrogen (N-5) on the porous carbon surface. The CO_2/N_2 selectivity of the sample is up to 11, and no obvious decrease in the CO_2 uptake capacity was observed even after seven times cycles, which may be due to the physisorption and easy desorption of CO_2. Overall, the sugar-rich microalgae derived N-doped activated carbons show a promising application in CO_2

capture, and the micropore distribution and nitrogen functionalities should be taken careful consideration in the preparation of activated carbons.

Acknowledgements

We acknowledge financial supports provided by the National Natural Science Foundation of China (21406255).

References

1 H. H. Wu, R. S. Reali, D. A. Smith, M. C. Trachtenberg, J. Li, *Chem. Eur. J* ., 2010, **16**, 13951.
2 C. Azar, K. Lindgren, E. Larson, K. Mollersten, *Clim.Change,* 2006, **74**, 47.
3 R.S. Haszeldine, *Science,* 2009, **325**, 1644.
4 C.S. Song, *Catal. Today,* 2006, **115**, 2.
5 N. MacDowell, N. Florin, A. Buchard, J. Hallett, A. Galindo, G. Jackson, et al, *Energy Environ. Sci.,* 2010, **3**, 1645.
6 D. Wang, C. Sentorun-Shalaby, X. Ma, C. Song, *Energy and Fuels,* 2011, **25**, 456.
7 M. Sevilla and A. B. Fuertes, *Energy Environ. Sci.,* 2011, **4**, 1765.
8 Q. Wang, J. Luo, Z. Zhong, A. Borgna, *Energy Environ. Sci.,* 2011, **4**, 42.
9 A.R. Millward, O.M. Yaghi, *J. Am. Chem. Soc.,* 2005, **127**, 17998.
10 K. Sumida, D.L. Rogow, J.A. Mason, T.M. McDonald, E.D. Bloch, Z.R. Herm, *Chem. Rev.,* 2012, **112**, 724.
11 S. Keskin, T. M. Heest, D. S. Sholl, *ChemSusChem.,* 2010, **3**,879.
12 H. Furukawa, O. M. Yaghi, *J. Am. Chem. Soc.,* 2009, **131**, 8875.
13 J. T. Wang, S. Xu, Y. F. Wang, R. Cai, C. X. Lv, W. M. Qiao, D. H. Long, L. C. Ling, *RSC Adv.,* 2014, **4**, 16224.
14 X. Yang, M. Yu, Y. Zhao, C. Zhang, X.Y. Wang, J.X. Jiang, *J. Mater. Chem. A,* 2014, **2**, 15139.
15 A. Wahby, J. M. R. Fernández, M. M. Escandell, A. S. Escribano. J. S. Albero, F. R. Reinoso, *ChemSusChem.,* 2010, **3**, 974.
16 R. Z. Bai, M. L. Yang, G. S. Hu, L.Q. Xu, X. Hu, Z.M. Li, S.L .Wang, W. Dai, M.H. Fan, *Carbon*, 2015, **81**, 465.
17 M. S. Shafeeyan, W. M. A. Wan Daud, A. Houshmand, A.Arami-Niya, *Appl. Surf. Sci.,* 2011, **257**, 3936.
18 A. Grondein, D. Belanger, *Fuel,* 2011, **90**, 2684.
19 M. Sevilla, V. V. Patricia, B. Antonio, *Adv. Funct. Mater,* 2011, **21**, 2781.
20 G. P. Hao, W.C. Li, D. Qian, A.H. Lu, *Adv. Mater.*, 2010, **22,** 853.
21 W. Xing, C. Liu, Z.Y. Zhou, L. Zhang, J Zhou, S.P. Zhuo, Z.F Yan, H. Gao, G.Q. Wang, S.Z. Qiao, *Energy Environ. Sci.,* 2012, **5**, 7323.
22 Z. Q. Zhang, K. Wang, J. D. Atkinson, X.L. Yan, X. Li, M.J. Rood, Z.F. Yan, *J.Hazard.Mater.,*2012**, 229**, 183.
23 C. Falco, M. Sevilla, R. J. White, R. Rothe, M.M. Titirici, *ChemSusChem*, 2012, **5**, 1834.
24 M. Sevilla, W. Gu, C. Falco, M. M. Titirici, A.B. Fuertes, G. Yushin, *J. Power Sources*, 2014, **267**, 26.
25 J. Singh, S. Gu, *Renew. Sust. Energ. Rev.,* 2010, **14**, 2596.
26 G. Miao, C. C. Zhu, J. J. Wang, Z. C. Tan, L. Wang, L. Z. Kong, *Green Chem.,* 2015, **17**, 2538.
27 S. M. Heilmann, H. T. Davis, L. R. Jader, P. A. Lefebvre, M. J. Sadowskyd, F. J. Schendel, M. G. von Keitz, K. J. Valentas, *Biomass Bioenerg,* 2010, **34**, 875.
28 E. Raymundo-Pinero, M. Cadek, F. Beguin, *Adv. Funct. Mater,* 2009, **19**, 1032.
29 M. Sevilla, C. Falco, M. M. Titiricic, A. B. Fuertes, *RSC Adv,* 2012, **2**, 12792.
30 B. Hu, K. Wang, L.Wu, S. H.Yu, M. Antonietti, M. M Titirici, *Adv. Mater,* 2010, **22**, 813.
31 K. Gong, F. Du, Z. Xia, M. Durstock, L. Dai, *Science*, 2009, **323**, 760.
32 H.W. Liang, X.D. Zhuang, S. Bruller, X.L. Feng, K. Mullen, *Nat.* Commun, DOI: 10.1038/ncomms5973.
33 F. Kapteijn, J. A. Moulijn, S. Matzner, H. P. Boehm, *Carbon,* 1999, **37**,1143.
34 J. R. Pels, F. Kapteijn, J. A. Moulijn, Q. Zhu, K. M. Thomas, *Carbon*, 1995, **33**, 1641.
35 S. B. Deng, H.R. Wei, T. Chen, B. Wang, J. Huang, G. Yu, *Chem. Eng. J.,* 2014, **253**, 46.
36 G. K. Parshetti, S. Chowdhury, R. Balasubramanian, *Fuel*, 2015, **148**, 246.